

Inclusion Complexes between Cyclodextrins and Triblock Copolymers in Aqueous Solution: A Dynamic and Static Light-Scattering Study

Gustavo G. Gaitano[†] and Wyn Brown*

Department of Physical Chemistry, University of Uppsala, Box 532, S-751 21 Uppsala, Sweden

Gloria Tardajos

Departamento de Química-Física I, Universidad Complutense de Madrid, 28040 Madrid, Spain

Received: July 8, 1996; In Final Form: October 24, 1996[®]

Simultaneous static and dynamic light experiments have been made on various cyclodextrins and cyclodextrin derivatives, as well as the inclusion complexes formed between different polyethylene oxide/polypropylene oxide triblock copolymers (PEO–PPO–PEO) (plurionics) and dimethyl- β -cyclodextrin (DIMEB). The inclusion complexes formed between DIMEB and plurionics are highly soluble, in contrast to the insoluble complexes formed between β -cyclodextrin and the same substances. The static light-scattering (LS) data show that approximately 11 DIMEB molecules thread onto the copolymer chains and are located on the PPO block. With the inverse structure (PPO–PEO–PPO), about seven DIMEB molecules are present in the complex. NMR measurements are used to substantiate complex formation by means of characteristic changes in the proton signals. Hydrodynamic radii obtained from the dynamic LS data at infinite dilution for the cyclodextrins correspond well with dimensions determined using X-ray methods. Inverse Laplace transformation (ILT) allowed resolution of the relaxational modes from the cyclodextrin/pluronic complex and the excess cyclodextrin. The complexes formed with the DIMEB are shown to be significantly larger than the copolymer unimers, which may be due to accentuation of steric hindrance to flexing in the PPO block. With the inverse pluronic structure, on the other hand, the complex is smaller in radius than the unimer. At temperatures above which the copolymer forms micelles, addition of DIMEB inhibits both cluster formation and micellization of the plurionics and also prevents network formation with the inverse pluronic, whereas the trimethyl analogue (TRIMEB) does not have this effect.

1. Introduction

Cyclodextrins (CD) are cyclic oligosaccharides having 6, 7, or 8 glucopyranose units linked by glycosidic bonds α -1,4 (α , β , and γ -cyclodextrins, respectively). They have a toroidal or hollow, truncated cone shape with an apolar, hydrophobic interior and two hydrophilic rims formed by the primary (narrower rim) and secondary (wider rim) OH groups. Their unusual structures give the CDs the ability to form inclusion complexes through noncovalent interactions with molecules that fit into the cavity. Cyclodextrins are consequently of great interest in a variety of fields.¹

In this work we have studied the inclusion complexes between dimethylated β -CD and nonionic polymeric surfactants (polaxamers or plurionics). These amphiphiles are low molecular weight linear triblock copolymers of polyethylene oxide (PEO) and polypropylene oxide (PPO) (PEO–PPO–PEO or PPO–PEO–PPO). Their properties in solution are markedly dependent on the relative size, composition, and disposition of the blocks, and they have recently attracted great interest because of their utility and their complex aggregation behavior in aqueous solution. The plurionics have been studied thoroughly during recent years^{2,3} which provides a good framework for a study of the complexing interaction between CDs and plurionics. Many reports in the literature concern the complexes between CDs, either in the natural state or modified, and low molecular weight compounds.⁴ However, there are few papers dealing with polymers and their interactions with CDs. To our

knowledge, there are no studies using dynamic or static light scattering on these systems. In 1990 Harada et al.⁵ published the first report on complexation between CDs and polymers and found that α -CD forms solid complexes with poly(ethylene glycol)s (PEG) of low molecular weight (400–1000) but the PEGs do not with β -CD. Later on,^{6,7} they found that β -CD and γ -CD gave crystalline complexes with polypropylene glycol (PPG) and polyisobutylene (PIB) but not with PEG. Synthesis of “trapped” polymers in CDs^{8,9} has also been reported and, in recent papers, double-stranded inclusion complexes of γ -CDs with PEG.¹⁰ With the triblock copolymers dealt with here, there are the X-ray diffraction and NMR studies of Topchieva et al. on β -CDs and plurionics. These describe the formation of insoluble¹¹ and soluble¹² complexes of CDs. The latter complexes are strung along the polymer chain (depending on the size of the hydrophilic block), and the CDs have a preference for complexing with the hydrophobic PPO blocks.

We selected plurionics L81, P85, F87, and F88, in which the length of the middle PPO block is kept constant (39 PO units) and which differ only in the polymerization degree of the PEO moieties (6, 27, 67, and 96 EO monomers, respectively), with the aim of examining the effect on the complexation when the hydrophilic block length is increased. In addition, an inverse pluronic (25R8:PPO–PEO–PPO having 15 PO units in each wing and 156 EO units in the center) has been studied to examine the effect of changing the relative positions of the blocks. We have also examined pure PPOs and PEOs of different polymerization degrees. Owing to the selectivity of the cavity size of the CDs when forming complexes and their

[†] Permanent Address: Departamento de Química-Física I, Universidad Complutense de Madrid, 28040 Madrid, Spain.

[®] Abstract published in *Advance ACS Abstracts*, December 15, 1996.

high water solubilities, we have chosen the methylated derivatives of β -CD as the most suitable for the present light-scattering study.

2. Experimental Section

2.1. Chemicals. The triblock copolymers (plurionics L81, P85, F87, F88, and 25R8) were from BASF Wyandotte Corp., Parsippany, NJ. α -, β -, and γ -cyclodextrins were from Aldrich, as well as the methylated derivatives heptakis(2,6-di-*O*-methyl)- β -cyclodextrin (DIMEB) and heptakis(2,3,6-tri-*O*-methyl)- β -cyclodextrin (TRIMEB) with purities of 99% and 97%, respectively. 2-Hydroxypropyl- β -cyclodextrin was a gift from D. Veiga. PEOs and PPOs of different polymerization degrees came from Aldrich, Merck, Fluka, and Hercules Powder, Inc. All substances were used without further treatment. Solutions were prepared with freshly purified water (Millipore Super-Q-System) and stored overnight at 6 °C. They were filtered with 0.1 μ m filters (Anotop) directly into 5 mL cylindrical scattering ampules that were then sealed. The D₂O used for the NMR measurements came from Sigma, with a deuterated content of 99.9%.

2.2. Dynamic and Static Light Scattering. Simultaneous dynamic light-scattering (DLS) and static light-scattering (SLS) measurements were performed in the same apparatus (see also ref 1). The reduced scattered intensity Kc/R_θ has been obtained with an optical constant for vertically polarized light defined as

$$K = 4\pi n_0^2 (\partial n / \partial c)^2 / (N_A \lambda^4) \quad (1)$$

Here, $n_0 = 1.333$ is the refractive index of water, λ the wavelength of the incident light, and $\partial n / \partial c$ is the measured refractive index increment (0.133 ± 0.002 mL g⁻¹ at 25 °C for solutions of DIMEB and also the pure block copolymers and the mixtures). The Rayleigh ratio used for toluene was $R_{90} = 3.1 \times 10^{-5}$ cm⁻¹ (ref 13). The light source was a frequency-stabilized 488 nm Ar ion laser operating at 500 mW. The detection optics included a Glan-Thompson polarizer attached to a 4 μ m diameter monomodal fiber coupled to an ITT FW130 photomultiplier. The output was digitized by an ALV-PM-PD amplifier discriminator. The autocorrelator was an ALV-5000 digital multiple τ instrument with 288 exponentially spaced channels. The measuring cells were immersed in a thermostated bath of *trans*-decalin stable to within ± 0.02 °C in each run.

2.3. Data Analysis. The obtained intensity autocorrelation function, $g_2(t)$, is related to $g_1(t)$, the field correlation function, through the Siegert relation

$$g_2(t) = 1 + \beta |g_1(t)|^2 \quad (2)$$

where $0 < \beta \leq 1$ is a nonideality factor depending on the finite area of the fiber aperture. $g_1(t)$ can be written as the Laplace transform of the relaxation rate distribution, $G(\Gamma)$:

$$g_1(t) = \int_0^\infty G(\Gamma) e^{-\Gamma t} d\Gamma \quad (3)$$

Alternatively, this equation can be expressed in terms of relaxation times, τ

$$g_1(t) = \int_{-\infty}^\infty \tau A(\tau) e^{-t/\tau} d(\ln \tau) \quad (4)$$

Regularized inverse Laplace transformation analysis (RILT) is performed on the measured $g_2(t)$. The calculation was made using the algorithm REPES,¹⁴ employing the analysis package GENDIST.¹⁵ The relaxation time distributions are normalized

to unit area to facilitate comparisons and are given in the form of $\tau A(\tau)$ versus $\log \tau$, which provides an equal area representation.¹⁶ The curves were fitted over a relaxation time range between 0.5 μ s and 1 s, with densities of 18 points per decade. The default value for the "smoothing parameter", P , was 0.5 except when two peaks approach closely, in which case P was chosen as the maximum required to distinguish adjacent peaks. The relaxation rate, Γ , and the amplitude of each mode were calculated from the moments of the distributions. The translational diffusion coefficient was obtained as

$$D = \Gamma / q^2 \quad (q \rightarrow 0) \quad (5)$$

with q the scattering vector. All measurements were performed at 90°. In the limit of small concentrations

$$D = D_0(1 + k_D c + \dots) \quad (6)$$

c is the concentration, k_D the hydrodynamic virial coefficient, and D_0 the diffusion coefficient at infinite dilution. The hydrodynamic radius, R_h , is obtained through the Stokes-Einstein equation:

$$R_h = \frac{k_B T}{6\pi\eta_0 D_0} \quad (7)$$

where η_0 is the viscosity of the solvent, T the absolute temperature, and k_B the Boltzmann constant.

2.4. ¹H NMR Measurements. All samples were prepared in 0.7 mL of D₂O as solvent, containing about 10 mg of polymer, and an amount of CD according to the molar ratio. ¹H NMR spectra were taken up in a Varian Unity 400 instrument at 400 MHz for ¹H, fitted with a thermostating unit. All measurements were carried out at 25 ± 0.5 °C and treated in a Sun Sparc workstation. The chemical shifts are relative to the HDO signal, taken as 4.63 ppm.

3. Results and Discussion

Addition of β -CD at a concentration of 0.012 M (1.36%) to dilute solutions (less than 3%) of L81, P85, F87, F88, 25R8, and PPOs of different polymerization degrees ($M_w = 790, 1220$, and 2000) led in each case to precipitation of a white powder. Precipitation was immediate with L81, PPO, and 25R8 but slow (several hours) with the other pluronic copolymers. According to Topchieva et al.,¹⁷ working with β -CD and similar plurionics, the precipitates formed are solid inclusion complexes of the β -CD and the polymeric chains. No precipitation was observed, however, when β -CD was added to solutions containing different chain lengths of PEO ($M_w = 1000, 2000, 4000, 6000, 12000$). This observation agrees with the results obtained by Harada et al.¹⁸ for PEO together with cyclodextrins. β -CD has an appropriate cavity size for the hydrophobic PO units, but it is too wide to form complexes with the hydrophilic and less bulky EO units (although α -CD forms insoluble complexes in high yield with PEOs of molecular weight less than 1000). Precipitation of the complexes, together with the low solubility of pure β -CD (1.85 g L⁻¹) itself, effectively prevents a light-scattering study, so we focused our attention on the much more soluble methylated derivatives of β -cyclodextrin: DIMEB and TRIMEB.

Studies with DIMEB and TRIMEB. *Size and Shape of Cyclodextrins.* Simultaneous static and dynamic light-scattering measurements were initially made on several pure cyclodextrins in aqueous solution. Despite the very small size of the cyclodextrins, which stretches the practical limit of the light-scattering technique, use of a high laser intensity (0.5 W) made

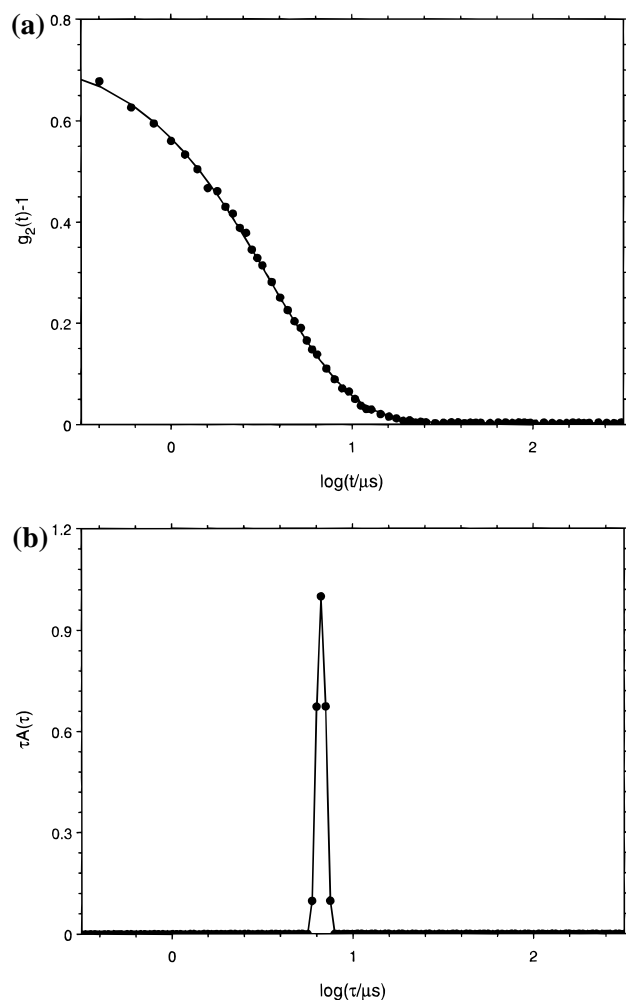


Figure 1. (a) Autocorrelation function for DIMEB 5% at 25 °C and (b) corresponding inverse Laplace transform (ILT).

it possible to obtain a surprisingly good correlograms as shown in Figure 1a for a solution of dimethyl- β -cyclodextrin (DIMEB), which is the main subject of this study. The corresponding inverse Laplace transform (ILT) result using REPES is illustrated in Figure 1b. The relaxation rates, Γ , obtained from the peak moments were determined as a function of scattering vector q and shown to have a linear dependence, passing through the origin and defining a diffusive process. Figure 2a shows the dependence of the diffusion coefficients for DIMEB at three temperatures. Combining the infinite dilution intercepts (D_0) with the viscosity of water (η_0) at the appropriate temperature in the Stokes–Einstein equation yields the hydrodynamic radius R_h . The value $R_h = 7.9 \text{ \AA}$ was obtained independently of temperature. We note here that for particles larger than the solvent molecules, the factor 6π in eq 7 is appropriate, whereas for diffusing particles only slightly larger than or approximately equal to the size of the solvent molecules, the factor should be replaced by 4π . We refer to the studies of Amu for a more detailed discussion.¹⁹ A common feature of the data is the characteristic negative values of the hydrodynamic virial coefficient, k_D . The latter is defined by

$$k_D = 2A_2M - k_f - 2v_2 \quad (8)$$

where A_2 is the second virial coefficient, M the molar mass, k_f the concentration-dependent friction factor, and v_2 the solute partial specific volume. The negative k_D derives from the negative second virial contributions at all temperatures studied (see below, Figure 5). The dependence of k_D on temperature

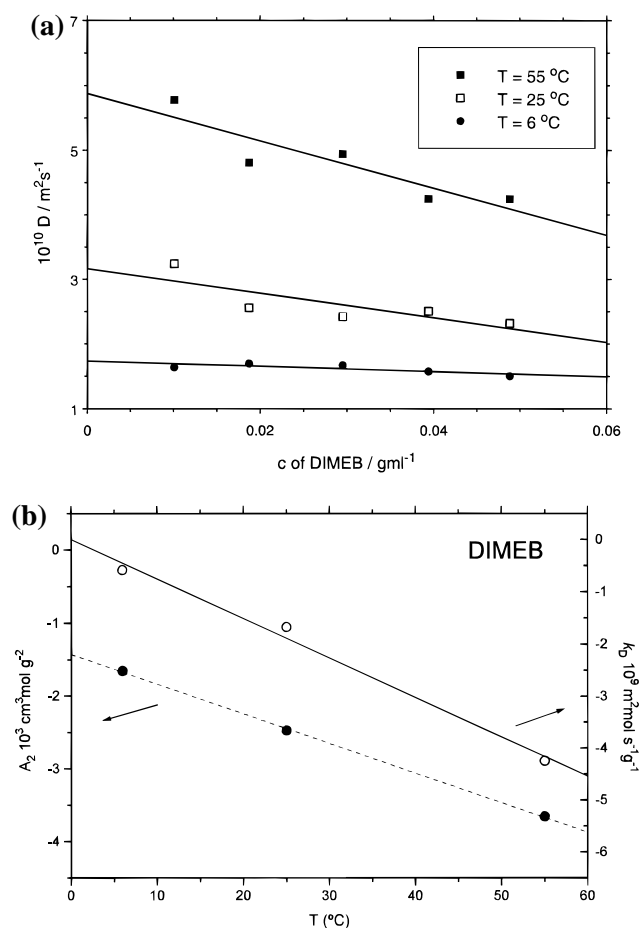


Figure 2. (a) Diffusion coefficients of DIMEB versus concentration at 6, 25, and 55 °C. (b) Second virial coefficient, A_2 , and hydrodynamic virial coefficient k_D as a function of temperature.

is compared with that of the second virial coefficient in Figure 2b and illustrates this point.

The obtained hydrodynamic radii for the other cyclodextrins given in Figure 3 are also reasonable in light of the known dimensions from X-ray diffraction, CPK (Corey–Pauling–Koltun) models based on hard spheres with van der Waals radii, and the internal cavity dimensions^{20,21} (See Table 1). For the β -CD, the intensity contribution from the nonassociated cyclodextrin was extremely small, owing to the presence of large clusters in the solutions. Typical data are illustrated in Figure 4a for β -cyclodextrin using two filter densities. The 0.02 μm Anotop filter removes the aggregates, but the intensity of the remaining peak is very small (intensity contribution $\leq 1\%$). Here, the peaks are shown with the same height to facilitate comparison. The apparent hydrodynamic radius estimated from the relaxation time of the slower peak in Figure 4a is 102 nm. The size of the clusters was also estimated by examining the angle dependence of the inverse intensity of the solution filtered through the 0.2 μm filter as shown in Figure 4b. This is possible, since the distribution is essentially single-modal. The value $R_g \approx 165 \text{ nm}$ was obtained. That the corresponding diameter is comparable to (or exceeds) the filter cutoff possibly reflects further aggregation occurring after filtration during equilibration prior to measurements. Coleman et al.²² have examined the aggregation behavior of the cyclodextrins using light scattering and found a cluster size of 210 nm for β -cyclodextrin. These workers concluded that the solubility is related to the interaction of the aggregate structure with that of water. They, however, found that α - and γ -cyclodextrins are also extensively associated in solution, in contrast to the present study where we only observe a very small relative amount of a

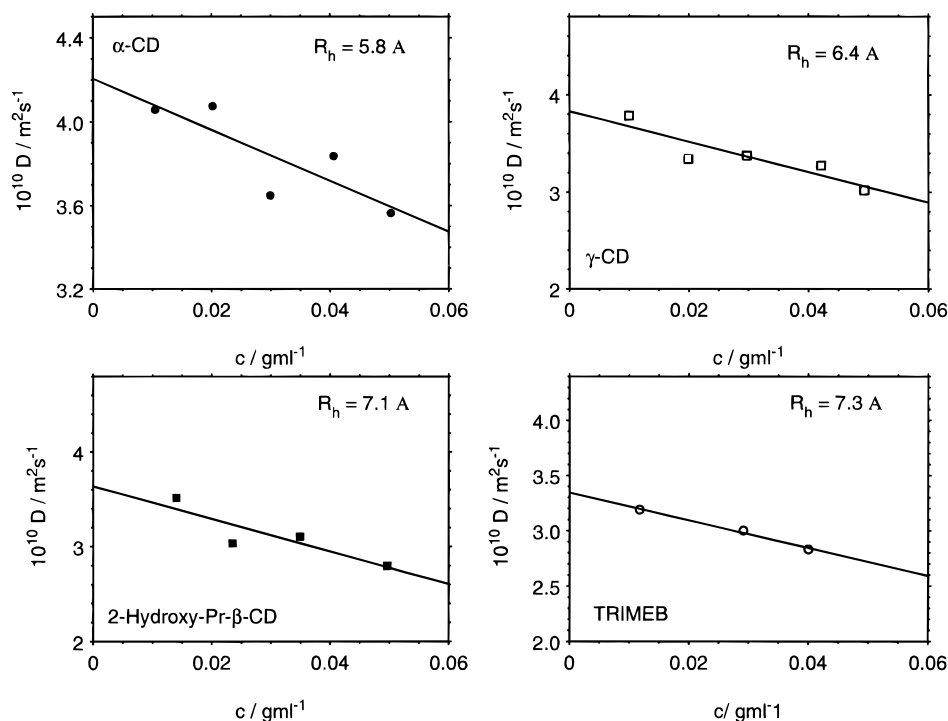


Figure 3. Diffusion coefficients and calculated R_h for several CDs.

TABLE 1: Measured R_h and Molecular Weights of CDs at 25 °C

cyclodextrin	M_w	width, height (Å) ^c	measured M_w	R_h (Å)
α-CD	972.86	13.7, 7.9	850	5.8
β-CD ^a	1131.01	15.3, 7.9		6.2
γ-CD	1297.15	16.9, 7.9	1350	6.4
DIMEB	1331.4	15.3, 10.9	1250	7.9
TRIMEB	1429.57	15.3, 10.9	1250	7.3
2-hydroxypropyl-β-CD ^b	~1400	15.3, 14.7	1650	7.1

^a See text. ^b Random substitution of 4.6 sites of the CD. ^c Using CPK, the space-filling sphere models.

cluster component. These workers did not report values for the sizes of nonassociated CDs. We also note that Coleman et al. found an apparent diameter of 40 Å for DIMEB, i.e., it is apparently associated. The effective radius is thus substantially greater than the hydrodynamic radius of 7.9 Å found in the present work. Furthermore, at high pH (12.5) on ionization of the hydroxyl groups, however, they found an apparent diameter of 20 Å for β-cyclodextrin, and this value might have been expected to correspond to the nonassociated material. However, the present measurements gave $R_h = 6.2$ Å for β-CD, which is a reasonable value compared with 7.9 Å for DIMEB, taking into account the bulk of the additional methyl groups at the rims of the molecule.

We have also used the total intensities measured simultaneously in the light-scattering experiments to calculate the molar masses of the cyclodextrins. Typical data are illustrated in Figure 5 for DIMEB at the three temperatures of Figure 2a. The average M_w is close to 1200, which agrees well with the theoretical value of 1331 for the seven-membered glycosidic ring and confirms the monomeric nature of the cyclodextrin. The second virial coefficients are negative for the binary cyclodextrin/D₂O systems at the temperatures studied (see also the negative slopes in Figures 2a and 3), reflecting very weak thermodynamic interactions with water. Moreover, A_2 becomes more strongly negative with increasing temperature as shown in Figure 2b, in agreement with the decreasing solubility as T is increased. The molar masses obtained for the other cyclo-

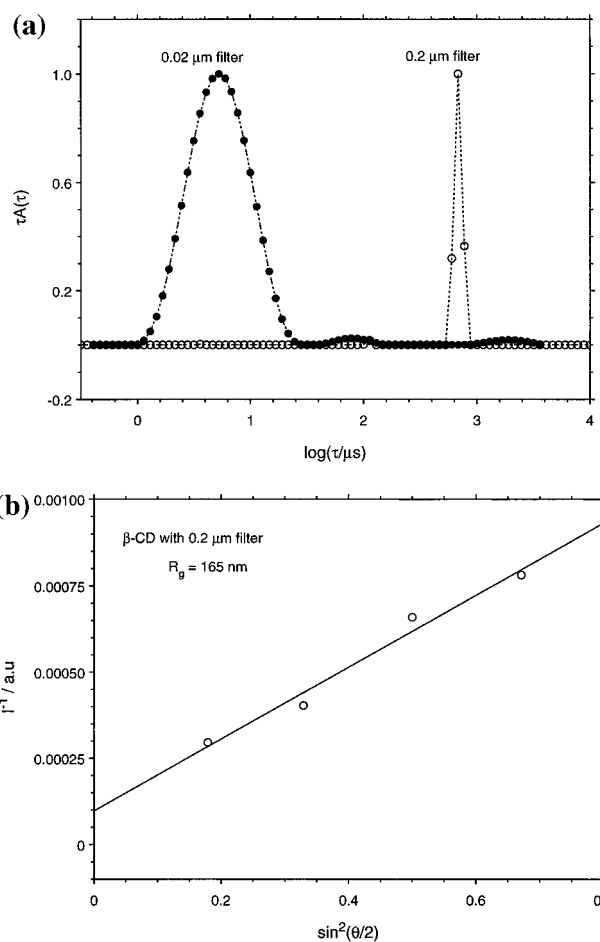


Figure 4. (a) Relaxation time distributions for β-CD 1.3% at 25 °C with filters of 0.02 and 0.2 μm. (b) Angle dependence for β-CD 1.3% at 25 °C filtered with 0.2 μm filter showing the radius of gyration of the aggregates.

dextrins in Figure 6 are in good agreement with the theoretical values (see also Table 1).

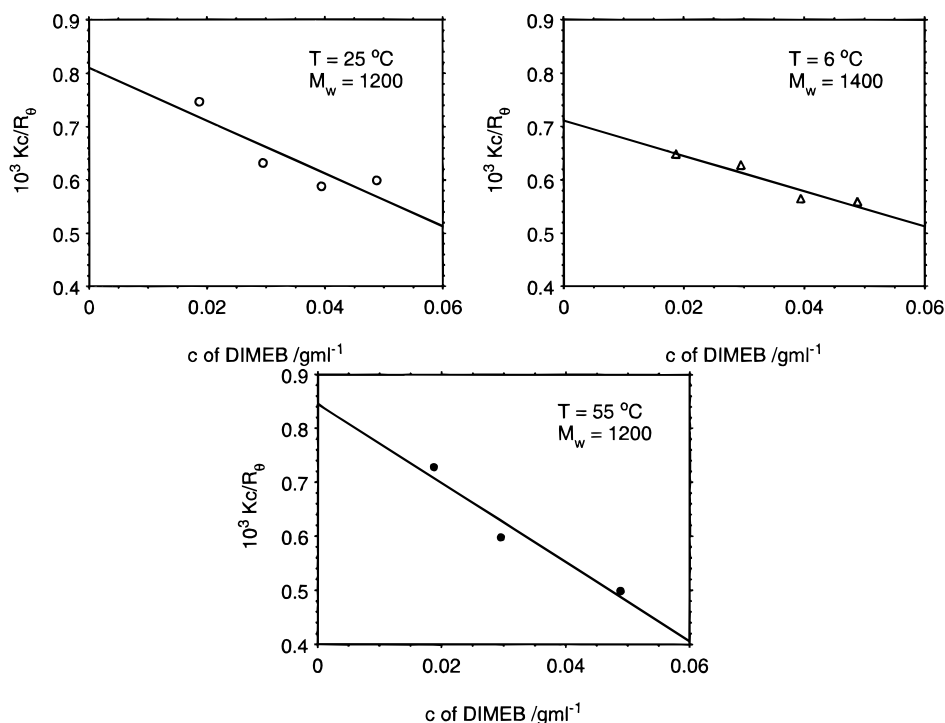


Figure 5. Concentration dependence of intensity light-scattering data for DIMEB at 6, 25, and 55 °C with the calculated M_w .

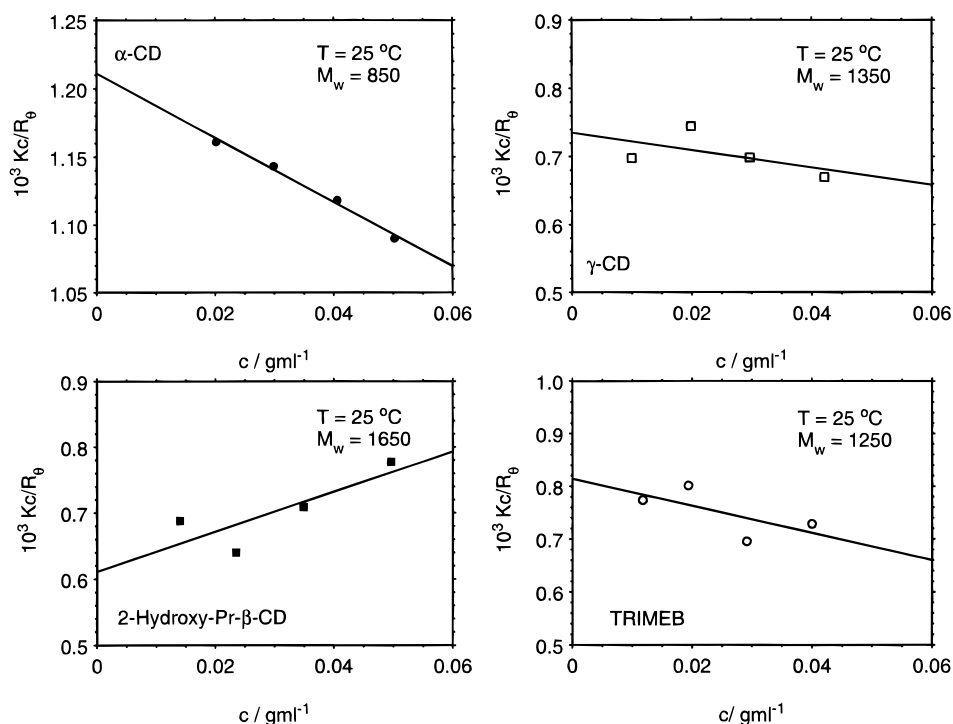


Figure 6. Concentration dependence of intensity light-scattering data for several CDs at 25 °C with the calculated M_w .

(PEO-PPO-PEO) L81. Pluronic L81 ($M_w = 2700$) is a relatively hydrophobic triblock copolymer, with a central block of 39 units of PO and two outer PEO blocks of 6 EO units. The strong overall hydrophobic character derives from the PPO block, which is large in comparison with the hydrophilic parts. This material was used in a previous work.²³ Figure 7a shows the intensity autocorrelation function $g_2(t)$ at angle 90° for pure L81 (1%) and for L81 with DIMEB and TRIMEB at 16 °C at a molar ratio $R = 5$ (CD:L81), together with the corresponding relaxation time distributions in Figure 7b. At 16 °C, pure L81 in aqueous solution shows phase separation of the LCST type (see ref 23 for details), as evidenced by the turbidity of the

solution in the measuring cell and by the presence of the slow relaxational mode in $g_2(t)$. In the presence of DIMEB, at the same temperature, clear solutions are obtained that only become turbid when the temperature is raised by several degrees, depending on the amount of cyclodextrin present. On the other hand, the trimethyl derivative, TRIMEB, when added to L81 solutions, did not give clear solutions (and there was even an increase in the turbidity). The increase in solubility with DIMEB is most probably due to the formation of a complex between L81 and the DIMEB. It is well-known that the solubility of various small molecules is enhanced in the presence of CDs.^{24,25} At temperatures and concentrations below phase

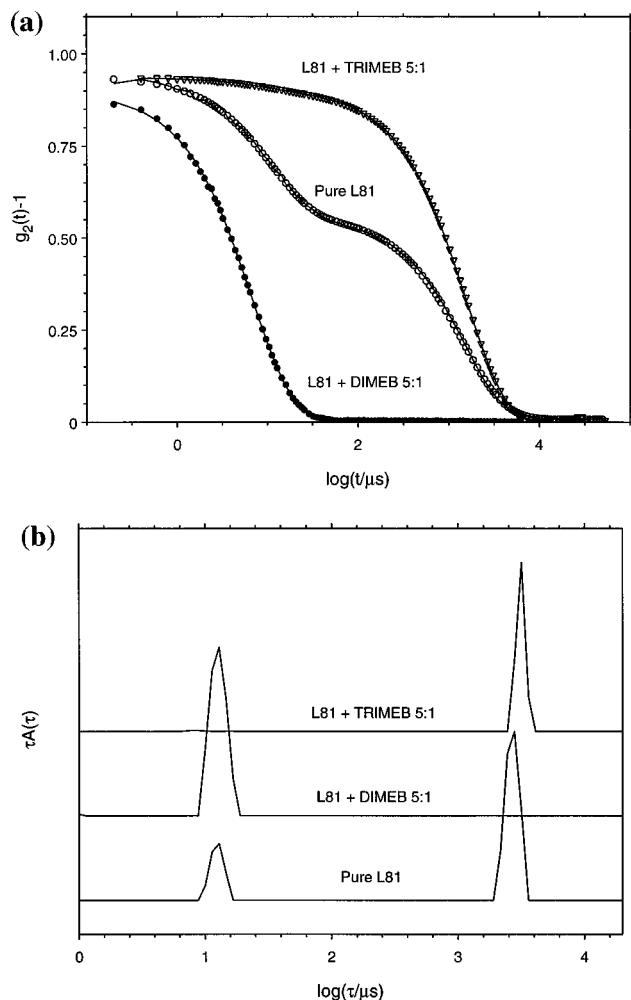


Figure 7. (a) DLS correlograms for L81 1% at 16 °C in presence of DIMEB and TRIMEB at molar ratio 5:1. (b) ILT for the curves of (a)

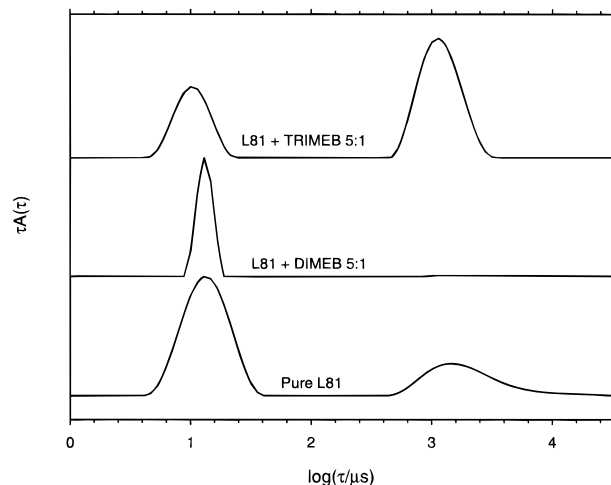


Figure 8. Relaxation time distributions for L81 1% at 14 °C in presence of DIMEB and TRIMEB at molar ratio 5:1.

separation, for example for L81 at 14 °C, addition of DIMEB leads to the disappearance of the clusters, which are a typical feature of most pluronics in solution at low temperatures and which lead to slow relaxational modes (Figure 8). These clusters are probably formed by residues of PPO and diblock copolymers from the synthesis, and their presence seems to be a ubiquitous feature of ethylene oxide-containing systems.^{26,27} Owing to the large size of the clusters, their contribution to the overall scattered intensity is high compared with that from the unimer.

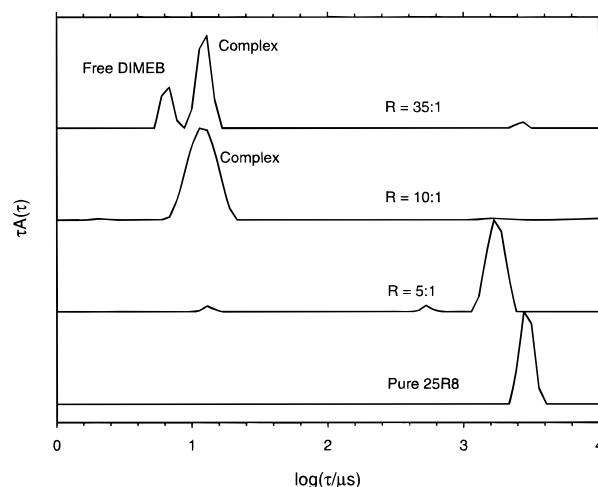


Figure 9. Relaxation time distributions for 25R8 + DIMEB at 40 °C at different molar ratios 25R8:DIMEB.

Although the clusters are few in number, the scattered intensity scales with the number of particles by c and is also proportional to r^6 , where c is the concentration and r is the radius of the particle. The scattering is thus dominated by the slower component. DIMEB is able to break these clusters not only with the L81 but also with the other pluronics studied. We note, however, that TRIMEB does not break the clusters. Unfortunately, the hydrodynamic sizes of L81, DIMEB, and the complex formed between them are similar and dynamic light scattering does not allow differentiation of the components with sufficient accuracy. This precludes estimation of the hydrodynamic radius of the complex in this system.

PPO-PEO-PPO 25R8. The “inverse” pluronic 25R8 ($M_w = 8550$) is a triblock copolymer having a central PEO block (156 EO units) and two PPO blocks at each end (15 PO units in each chain). The phase behavior and structures of 25R8 in solution have been examined previously.²⁸ At concentrations lower than 15% w/w and at temperatures below 35 °C only the unimer is present. At higher temperatures and concentrations, association between the PPO moieties in aqueous solution leads to polydisperse suspensions of network clusters of different size.²⁸ Figure 9 shows the ILT of the autocorrelation functions for 2% 25R8 at 40 °C for several molar ratios of DIMEB to 25R8. At $R = 0$ (pure 25R8) network structures are present at this temperature and give a slow mode with high scattered intensity. At $R = 5$ the total scattered intensity diminishes and a small fast mode appears. At $R = 10$ the network present in the absence of DIMEB does not form and only the mode due to the complex is observed. At $R = 35$ free DIMEB is present in excess, yielding a fast mode in addition to the complex. The double-peaked distribution was confirmed using pulsed field gradient NMR,³¹ which revealed the presence of two components. Significantly, addition of TRIMEB does not inhibit formation of the network, and we recall that with L81 the clusters also did not disappear with TRIMEB addition. At the lower temperature of 25 °C, pure 25R8 in solution does not form networks and only the mode due to the unimer is present. The diffusion coefficient for 25R8 at infinite dilution corresponds to $R_h = 32$ Å. When the molar ratio DIMEB:25R8 is increased, the complex has an apparent smaller size, as shown by the small but significant decrease in R_h (Figure 10). To verify if this decrease is real or simply due to changed interactions, DIMEB + 25R8 at constant molar ratio 25:1 was diluted at 25 °C. The diffusion coefficients for the complex extrapolated to zero concentration (see Figure 11) yield $R_h = 26.4$ Å, i.e., a

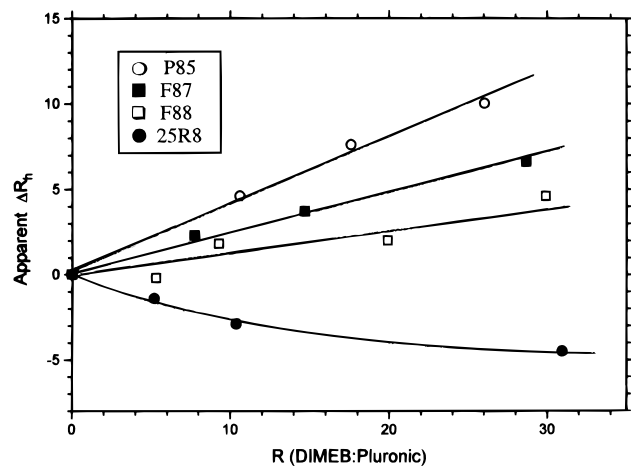


Figure 10. Increments of the apparent R_h for the complex (with reference to the unimer) versus the molar ratio DIMEB:pluronic.

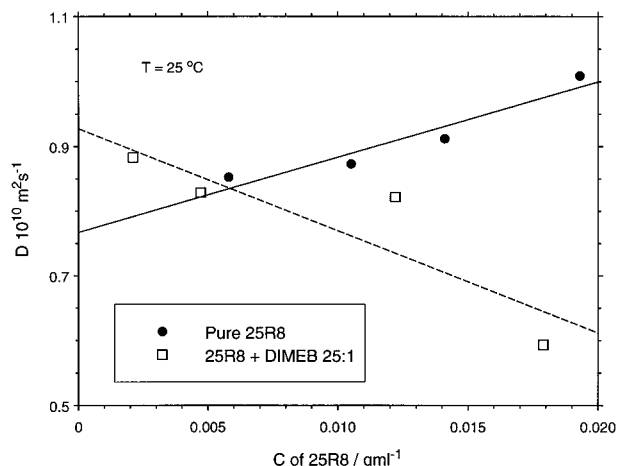
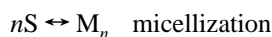


Figure 11. Diffusion coefficients for pure 25R8 and for the complex ($R = 25:1$) as a function of concentration at 25 °C.

decrease in size of 5.6 Å on complexation compared to pure 25R8 in solution.

PEO-PPO-PEO Block Copolymers P85, F87, and F88. These three pluronic block copolymers ($M_w = 4600, 7700$, and 10800) have in common a central PPO block of 39 PO monomers. The PEO blocks have, respectively, 27, 67, and 96 EO units.²³ The hydrophilic character increases according to the PEO block length. Their aggregation behavior is rather complex, but many of these compounds have in common the ability to form micelles when the temperature is increased.²⁹ The micelles typically have a core formed by the association of the PPO middle blocks and a concentric shell of PEO blocks (owing to the very short PEO blocks, L81 does not form micelles). Clusters of well-defined size are present in the dilute solutions at room temperature, but when the temperature is raised, the more hydrophobic components become included in the micellar cores. In solutions of typical surfactants, (e.g., SDS, alkyltrimethylammonium halides, etc.), the addition of cyclodextrins displaces the cmc by an amount equal to that of the CD present (if the stoichiometry is 1:1),³⁰ since there is a competitive equilibrium between micellization and complexation resulting in the formation of the complex S:CD:



With pluronic surfactants, qualitatively similar behavior is expected throughout the series. With pure P85 in solution at

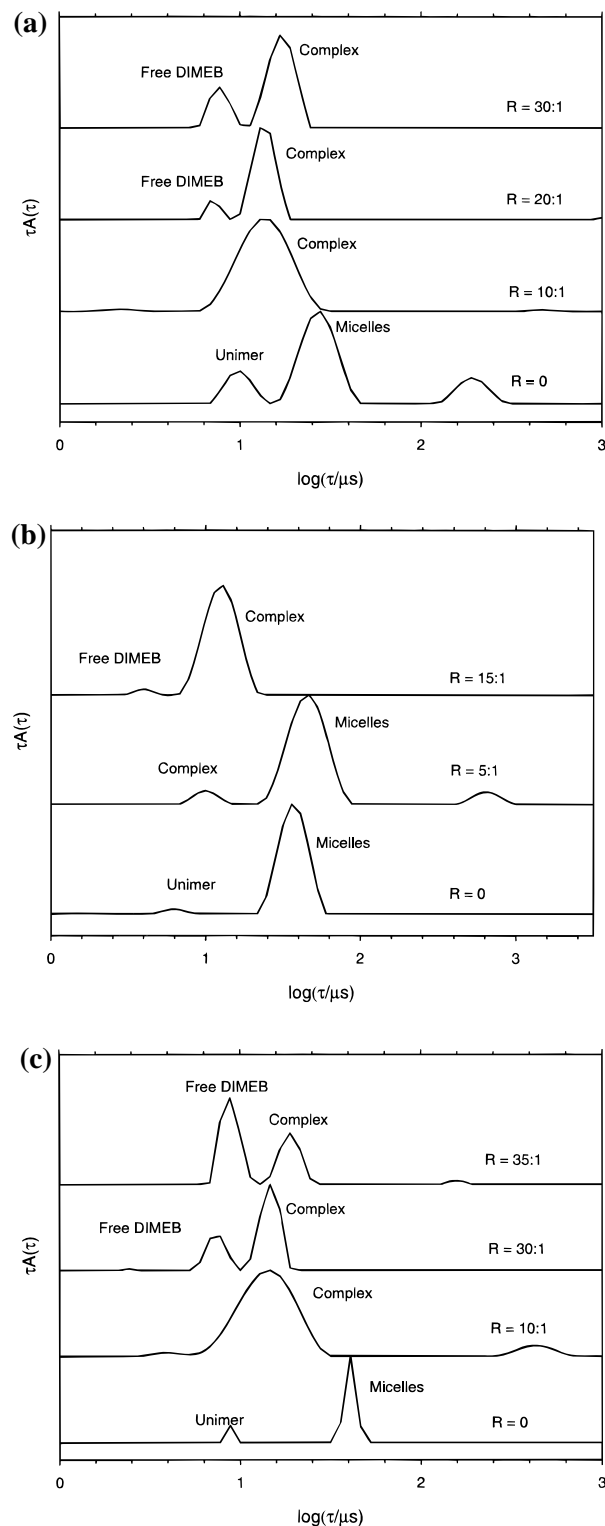


Figure 12. Relaxation time distributions at different molar ratios of (a) P85 + DIMEB at 25 °C, (b) F87 + DIMEB at 40 °C, and (c) F88 + DIMEB at 40 °C.

25 °C unimers and micelles coexist, whereas micelles form above a concentration of 1% at 40 °C. With F87 and F88 the cmc's are higher and micelles form above 32 and 36 °C, respectively, at a concentration of 5%. Parts a–c of Figure 12 show the effect of DIMEB on the relaxation time distributions. In these systems, the addition of DIMEB inhibits the formation of micelles. Thus, the relaxation mode due to micellar diffusion in the pure pluronic solutions disappears and only the modes due to diffusion of the complex and the free DIMEB when

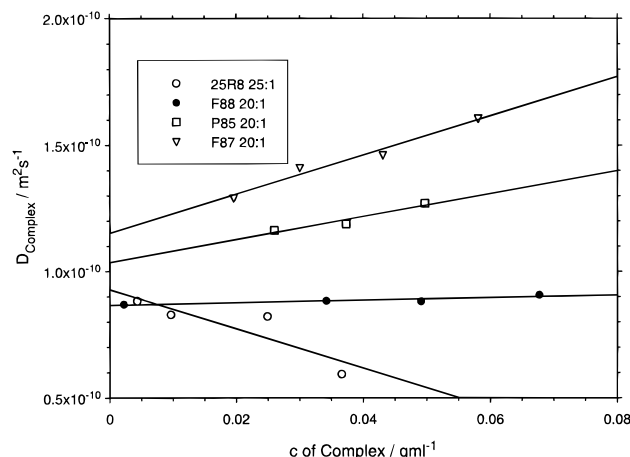


Figure 13. Diffusion coefficients for the complexes between DIMEB and pluronics versus the concentration of complex.

present in excess are observed. Again, the presence of the two peaks at high R values was confirmed using PFG NMR. However, TRIMEB inhibits neither micelle formation nor the formation of clusters. When the apparent hydrodynamic radii are plotted versus the molar ratio, there is a small increase in R_h with the amount of DIMEB present, i.e., there is an increase in R_h when the unimer is complexed to CD. This trend is more marked for P85 than for F87 and, in turn, for F88 (Figure 10). To obtain the complex size in the absence of interactions, it is necessary to extrapolate D for the mixtures at constant ratio to infinite dilution as was done for 25R8. Figure 13 shows the diffusion coefficient for the complex as a function of the complex concentration (determined as described below). The radii obtained from the zero-concentration D values using eq 7 show that the changes in the size of the unimer when complexed with DIMEB are small but significant. A similar conclusion was reached on the basis of the self-diffusion coefficients measured employing pulsed field-gradient NMR³¹ (for example, for P85, F87, and F88 at molar ratio of 10:1, the differences with respect to the unimer at $C = 1\%$ were 9.8, 6, and 13.4 Å).

(a) *Static Light Scattering (SLS)*. It is possible to estimate the stoichiometry (S) of the complexes by SLS measurements. When there is excess DIMEB and the modes of the free CD and the complexed unimer can be resolved, the overall intensity may be apportioned into the contributions of the DIMEB and of the complex by the normalized relative areas of the distributions given by

$$I_{\text{DIMEB}} = I \int_{\text{DIMEB}} \tau A(\tau) d(\log \tau) \quad (9a)$$

$$I_{\text{complex}} = I \int_{\text{complex}} \tau A(\tau) d(\log \tau) \quad (9b)$$

Here, I is the total averaged intensity. The GENDIST program gives the values of the integrated and normalized distributions. The intensity corresponding to the fast mode, I_{DIMEB} , is a measure of the concentration of free DIMEB (denoted c_{DIMEB}^f). In the Zimm equation

$$\frac{Kc_{\text{DIMEB}}^f}{R_{\theta=90}} = \frac{1}{M_w} + 2A_2c_{\text{DIMEB}}^f \quad (10)$$

the molecular weight is fixed to the known value for DIMEB (1331.4 g mol⁻¹). R_{90} is calculated using the intensity for the free DIMEB. The value of $\partial n/\partial c$ used in the calculation of K was taken as that of pure DIMEB in aqueous solution at 25 °C (0.133 mL g⁻¹). The second virial coefficient for the respective

ternary solution was obtained using the intensity of the free DIMEB calculated from the total intensity apportioned between the two modes using the relative amplitudes from the DLS experiment. Use of the virial coefficient calculated in this way this should not introduce substantial error, since alternative use of the A_2 for the binary DIMEB solutions gave similar values of S . The concentration of free DIMEB may then be determined using the following rearrangements in terms of the stoichiometry S :

$$S = \frac{c_{\text{DIMEB}}^b M_{\text{pluronic}}}{c_{\text{pluronic}} M_{\text{DIMEB}}} \quad (11)$$

where the concentrations, c , are expressed in g/mL. The concentration of the complexed DIMEB follows from

$$c_{\text{DIMEB}}^b = c_{\text{DIMEB}}^t - c_{\text{DIMEB}}^f \quad (12)$$

Superscripts b, t, and f refer, respectively, to bound, total, and free concentrations. Substituting the complexed cyclodextrin in eq 11 with eq 12 and r the ratio of molecular weights gives

$$c_{\text{DIMEB}}^f = c_{\text{DIMEB}}^t - S c_{\text{pluronic}}/r \quad (13)$$

This result is substituted in the Zimm equation to obtain a straight line from the slope from which the stoichiometry can be obtained:

$$r \left(c_{\text{DIMEB}}^t - \frac{1}{M_w(K/R - 2A_2)} \right) = S c_{\text{pluronic}} \quad (14)$$

Parts a and b of Figure 14 show fits to eq 14 for two different pluronics, and Table 2 gives the stoichiometries for P85, F87, F88, and 25R8. The average number of CDs per molecule of polymer is approximately the same for the pluronics with the same middle PPO block length (about 11 CD molecules), and it does not change with the temperature. However, from the stoichiometry values for F88 in Table 2, there would appear to be a systematic increase in S with the amount of excess DIMEB. For 25R8, there are approximately seven complexed DIMEB molecules per copolymer chain.

(b) *¹H NMR*. High-field NMR measurements can provide information on the location of the cyclodextrin molecules. Thus, in the presence of F88 at different molar ratios, characteristic changes in the chemical shifts for the interior protons H3 and H5 of DIMEB are observed, but there are no changes for the outer H1 protons. There are analogous changes in the shifts for the protons of the methyl group of the PO moiety. Here, shifts of -0.030 ppm are observed. In light of the extensive literature on NMR studies of such complexes, these shifts constitute direct evidence for the formation of an inclusion complex with the DIMEB.³² We note that Topchieva et al.^{11,12,33} only refer to the proton shifts of the pluronic itself. It is reasonable to expect that these correspond to the necklace-shaped structures found in the solid and soluble complexes formed between the various cyclodextrins and polymers.^{11,33} The simultaneous changes in the chemical shifts of the methyl protons of the PO moiety (and also with PPO itself—see below) show that the DIMEB preferentially locates on the PPO middle block. In mixtures of DIMEB and pure PEO ($M_w = 4000$), no changes were observed in the chemical shifts of the protons of either the CD or the PEO.

Polymers PPO and PEO. To further our understanding of the complexing action between cyclodextrins and these triblock copolymers, it is relevant to examine the interactions between DIMEB and the individual polymers PEO and PPO having comparable molecular size. With PPOs of $M_w = 790, 1200,$

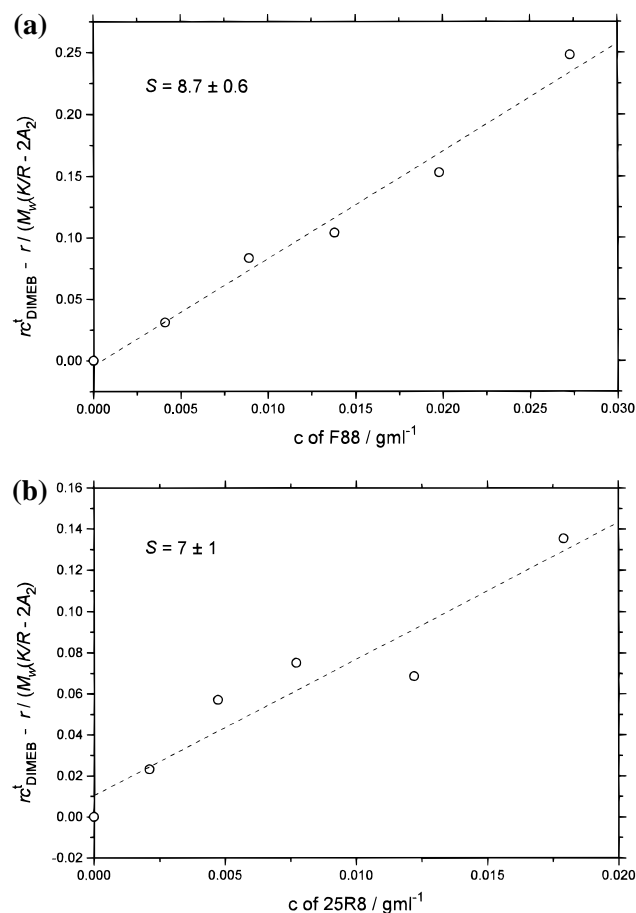


Figure 14. Calculation of the stoichiometry of the complexes according to eq 14 at 25 °C for (a) F88 + DIMEB at $R = 20:1$ and (b) 25R8 + DIMEB at $R = 25:1$.

TABLE 2: ΔR_h (Complex–Unimer) and Stoichiometries S of the Complexes with DIMEB

pluronic	ΔR_h (Å)	S
25R8	-4.5	7 ± 1 (25 °C, $R = 25:1$)
P85	5.4	10 ± 1 (25 °C, $R = 20:1$)
F87	4.7	13 ± 4 (25 °C, $R = 30:1$)
F88	0	8.7 ± 0.6 (25 °C, $R = 20:1$) 11.1 ± 0.4 (25 °C, $R = 30:1$) 12.6 ± 2.0 (40 °C, $R = 35:1$)

and 2000 at temperatures at which phase separation is observed for the pure polymers in aqueous solution, the addition of DIMEB promotes solubilization of this hydrophobic polymer (see Figure 15), whereas TRIMEB does not. With PPO 790, the sizes of DIMEB and the PPO chains are too close for resolution of the peaks in DLS. However, by plotting $Kc/R_{\theta=90}$ versus the concentration of DIMEB in the case of the pure DIMEB and in the additional presence of PPO ($M_w = 790$), keeping the molar ratio 7:1 constant, one notes strongly different concentration dependences of the curves (Figure 16). This difference reflects the binary interactions between DIMEB and PPO rather than the addition of the individual contributions from PPO and DIMEB, since the intensity of PPO is very small compared with the intensity contribution of DIMEB. In the calculation we have used a value of $\partial n/\partial c = 0.133 \text{ mL g}^{-1}$; i.e., the value is the same as for solutions of pure DIMEB and is also fortuitously the same as for these block copolymers in aqueous solution. Nothing can be said about the M_w of the complex, however, since it would be necessary to know the complex concentration, and also the two modes (DIMEB and complex) overlap. ^1H NMR measurements on solutions of PPO 790 and DIMEB also show similar and characteristic changes

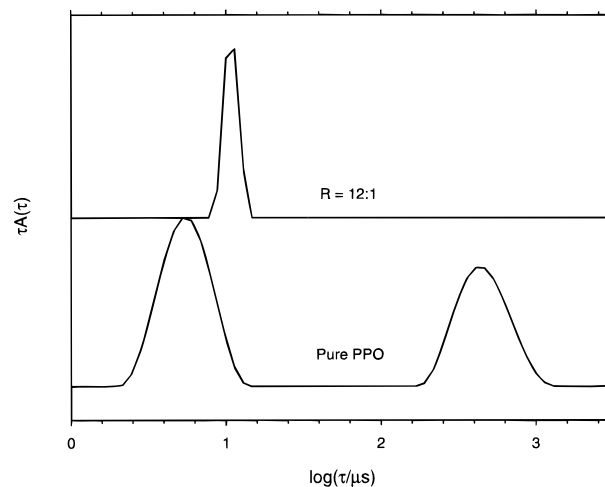


Figure 15. Relaxation time distributions at 25 °C for PPO 1% ($M_w = 790$) in presence and in absence of DIMEB.

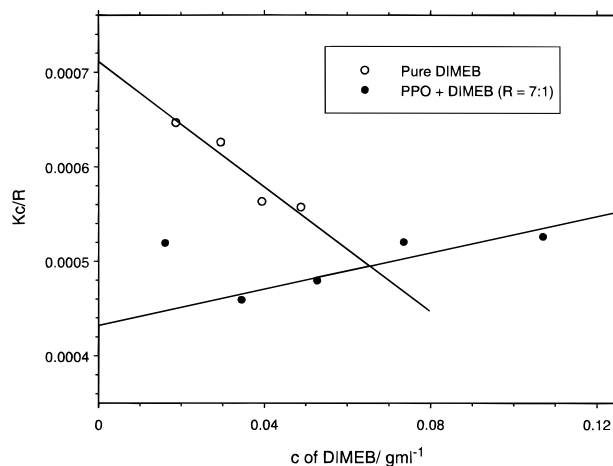


Figure 16. Concentration dependence of intensity light-scattering data at 6 °C for pure DIMEB and DIMEB + PPO 1% ($M_w = 790$) in molar ratio 7:1.

in the chemical shifts of the protons located in the interior of the CD cavity (H3 and H5) ($\Delta\delta = -0.079 \text{ ppm}$), as well as for the methyl protons of the PPO ($\Delta\delta = -0.065 \text{ ppm}$), while the H1 protons of the outer face of DIMEB remain unchanged. As with the pluronics, the DIMEB molecules thread onto the PPO chain. However, for PEOs of different polymerization degrees ($M_w = 1000, 2000, 4000, 6000$, and 12000), both DLS and SLS gave no evidence of interaction with either DIMEB or with TRIMEB.

4. Conclusions

Simultaneous SLS and DLS experiments have been made on the inclusion complexes formed between various pluronics and dimethylated β -cyclodextrin (DIMEB) as well as on individual pure cyclodextrins and polymers in solution. Sizes and molecular weights of the pure CDs (DIMEB, TRIMEB, α -CD, γ -CD, and 2-hydroxypropyl- β -CD) were determined in an initial phase, and the calculated values were found to be in good agreement with the known values. As is well-known, β -CD forms insoluble complexes with the pluronics as well as with PPO. However, P85, F87, and F88, form water-soluble complexes with DIMEB. Approximately 11 cyclodextrin molecules thread onto the copolymer and locate mainly on the center PPO block. This value does not change over the range of temperatures studied (6–55 °C). Furthermore, the addition of DIMEB inhibits association of pluronic unimers into micelles

or clusters. From the diffusion coefficients at infinite dilution, it is concluded that the complexes are significantly larger than the pluronic unimers, with relative changes in size that increase in the order P85 > F87 > F88. One may speculate that this is a consequence of steric hindrance to flexing motions of the PPO block by the mantle of cyclodextrin molecules.

The inverse pluronic structure, 25R8, when complexed with DIMEB, on the other hand, has a total of about seven cyclodextrins, a value that is consistent with the number of PO units in the chain (two wing blocks of 15 POs compared to the central block of 39 PO units for P85, F87, and F88). However, surprisingly, the size of the complex is then smaller than that of the unimer. One may attribute this contraction to a reduced tendency for PO block segregation in aqueous solution when the PO blocks have a mantle of cyclodextrin molecules providing them with a relatively hydrophilic surface. In contrast to the system without DIMEB, network formation through association of the hydrophobic PO moieties was not observed at 40 °C for 25R8 with DIMEB. For L81, although stoichiometries and sizes could not be determined owing to overlap of the DLS relaxational modes, solubilization of the copolymer under conditions that show phase separation for pure L81 and also the removal of clusters strongly suggest complexation. With the pluronics studied, TRIMEB on the other hand did not form complexes, as illustrated by its inability to inhibit phase separation and also its inability to inhibit micellization or to remove clusters. This may be due to the inhibition of hydrogen bonding owing to lack of OH groups at the rim of the cyclodextrin cavity, a possibility that remains with DIMEB.

Acknowledgment. The authors are indebted to Adolf Gogoll (Department of Organic Chemistry, Uppsala) for the ¹H NMR measurements, to Göran Svensk (Department of Physical Chemistry, Uppsala) for the refractive index increment measurements, and to Peter Stilbs (KTH, Stockholm) for providing the PFG-NMR data. We also thank Taco Nicolai, Le Mans, for valuable discussions. We acknowledge financial support from the Swedish Technical Research Council (TFR), from the M.E.C. of Spain through DGICYT Grant Nos. PB890113 and PB30448, and from the Vicerrectorado de Investigación of the Universidad Complutense (Madrid).

References and Notes

- (1) (a) Szelti, J. *Cyclodextrins and Their Inclusion Complexes*; Akademiai Kiado: Budapest, 1982. (b) Bender, M. L.; Komiyama, M. *Cyclodextrin Chemistry*; Springer-Verlag: Berlin, 1978.
- (2) Almgren, M.; Brown, W.; Hvidt, S. *Colloid Polym. Sci.* **1995**, 273, 2.
- (3) Mortensen, K. *J. Phys.: Condens. Matter* **1996**, 8, 1.
- (4) Saenger, W. *Angew. Chem., Int. Ed. Engl.* **1980**, 19, 344.
- (5) Harada, A.; Kamachi, M. *Macromolecules* **1990**, 23, 2823.
- (6) Harada, A.; Kamachi, M. *J. Chem. Soc., Chem. Commun.* **1990**, 1321.
- (7) Harada, A.; Li, J.; Suzuki, S.; Kamachi, M. *Macromolecules* **1993**, 26, 5267.
- (8) Wenz, G.; Keller, B. *Angew. Chem., Int. Ed. Engl.* **1992**, 31, 197.
- (9) Harada, A.; Okada, M.; Li, J.; Kamachi, M. *Macromolecules* **1995**, 28, 8406.
- (10) Harada, A.; Kamachi, M. *Nature* **1994**, 370, 126.
- (11) Topchieva, L. N.; Kolomnikova, E. L.; Banatskaya, M. I.; Kabanov, V. A. *Polym. Sci., Ser. A* **1993**, 35, 464.
- (12) Klyamkin, A. A.; Topchieva, I. N.; Zubov, V. P. *Colloid. Polym. Sci.* **1995**, 273, 520.
- (13) Moreels, E.; de Ceunink, W.; Finsy, R. *J. Chem. Phys.* **1987**, 86, 618.
- (14) Jakes, J. *Czech. J. Phys. B* **1988**, 38, 1305.
- (15) Schillén, K.; Brown, W.; Johnsen, R. M. *Macromolecules* **1994**, 27, 4825.
- (16) Nicolai, T.; Brown, W.; Johnsen, R. M.; Stepanek, P. *Macromolecules* **1990**, 23, 1165.
- (17) Topchieva, I. N.; Blyumenfel'd, A. L.; Klyamkin, A. A.; Polyakov, V. A.; Kabanov, V. A. *Polym. Sci.* **1994**, 36, 221.
- (18) Harada, A.; Kamachi, M. *Macromolecules* **1993**, 26, 5698.
- (19) Amu, T. *J. Chem. Soc., Faraday Trans. 1* **1979**, 75, 1226.
- (20) Song, L.; Purdy, W. C. *Chem. Rev.* **1992**, 92, 1457.
- (21) McMullan, R. K.; Saenger, W.; Fayos, J.; Mootz, D. *Carbohydr. Res.* **1973**, 31, 37.
- (22) Coleman, A. W.; Nicolis, I.; Keller, N.; Dalbiez, J. P. *J. Inclusion Phenom. Mol. Recognit. Chem.* **1992**, 13, 139.
- (23) Brown, W.; Schillén, K.; Hvidt, S. *J. Phys. Chem.* **1992**, 96, 6038.
- (24) Schlenk, H.; Sand, D. M. *J. Am. Chem. Soc.* **1961**, 83, 2312.
- (25) Lach, J. L.; Pauli, W. A. *J. Pharm. Sci.* **1966**, 55, 32.
- (26) Polik, W.; Burchard, W. *Macromolecules* **1983**, 16, 978.
- (27) Brown, W. *Polymer* **1985**, 26, 1647.
- (28) Mortensen, K.; Brown, W.; Jørgensen, E. *Macromolecules* **1994**, 27, 5654.
- (29) Brown, W.; Schillén, K.; Almgren, M.; Hvidt, S.; Bahadur, P. *J. Phys. Chem.* **1991**, 95, 1850.
- (30) Junquera, E.; Aicart, E.; Tardajos, G. *J. Phys. Chem.* **1992**, 96, 4533.
- (31) Gaitano, G. G.; Brown, W.; Stilbs, P. To be published.
- (32) Demarco, P. V.; Thakkar, A. L. *J. Chem. Soc., Chem. Commun.* **1970**, 2.
- (33) Polyakov, V. A.; Kolomnikova, E. L.; Topchieva, I. N.; Kabanov, V. A. *Polym. Sci., Ser. B* **1993**, 35 (5), 286.